



OPEN

## Experimental and modeling of solubility of *sitagliptin phosphate*, in supercritical carbon dioxide: proposing a new association model

Nedasadat Saadati Ardestani<sup>1</sup>, Seyed Ali Sajadian<sup>2,3</sup>✉, Nadia Esfandiari<sup>4</sup>, Adrián Rojas<sup>5,6</sup> & Chandrasekhar Garlapati<sup>7</sup>✉

The solubility of an anti-hyperglycemic agent drug, (R)-4-oxo-4-[3-(trifluoromethyl)-5,6-dihydro [1,2,4] triazolo[4,3-a] pyrazin-7(8H)-yl]-1-(2,4,5-trifluorophenyl) butan-2-amine (also known as *Sitagliptin phosphate*) in supercritical carbon dioxide (scCO<sub>2</sub>) was determined by an analytical and dynamic technique at different temperatures (308, 318, 328 and 338 K) and pressure (12–30 MPa) values. The measured solubilities were in the range of  $3.02 \times 10^{-5}$  to  $5.17 \times 10^{-5}$ ,  $2.71 \times 10^{-5}$  to  $5.83 \times 10^{-5}$ ,  $2.39 \times 10^{-5}$  to  $6.51 \times 10^{-5}$  and  $2.07 \times 10^{-5}$  to  $6.98 \times 10^{-5}$  in mole fraction at (308, 318, 328 and 338) K, respectively. The solubility data were correlated with existing density models and with a new association model.

### List of symbols

$A_1, B_1$	Eq. (6) Constants
$A_2, B_2$	Eq. (7) Constants
$A_3, B_3, C_3$	Eq. (8) Constants
$A_4, B_4, C_4$	Eq. (9) Constants
$A_5, B_5, C_5$	Eq. (10) Constants
$A_6, B_6, C_6, D_6, E_6, F_6$	Eq. (30) Constants
AARD%	Average absolute relative deviation percentage
$\hat{f}$	Fugacity in mixture
$H_{sol}$	Solvation enthalpy(kJ/mol)
$H_{sub}$	Sublimation enthalpy(kJ/mol)
$H_{total}$	Total enthalpy(kJ/mol)
$K_f$	Equilibrium constant
$M_{CO_2}$	Molar mass of CO <sub>2</sub> and drug (g/mol)
$M_{solute}$	Solute Molar mass
P	System pressure
$P^*$	Reference pressure
$P^s$	Sublimation pressure(Pa)
R	Universal gas constant, 8.314 J/(molK)
scCO <sub>2</sub>	Supercritical carbon dioxide

<sup>1</sup>Nanotechnology Research Center, Research Institute of Petroleum Industry (RIPI), 14857-336, Tehran, Iran. <sup>2</sup>Department of Chemical Engineering, Faculty of Engineering, University of Kashan, Kashan 87317-53153, Iran. <sup>3</sup>South Zagros Oil and Gas Production, National Iranian Oil Company, Shiraz 7135717991, Iran. <sup>4</sup>Department of Chemical Engineering, Marvdasht Branch, Islamic Azad University, Marvdasht, Iran. <sup>5</sup>Department of Science and Food Technology, Faculty of Technology, Packaging Innovation Center (LABEN), University of Santiago of Chile (USACH), Obispo Umaña 050, 9170201 Santiago, Chile. <sup>6</sup>Center for the Development of Nanoscience and Nanotechnology (CEDENNA), 9170124 Santiago, Chile. <sup>7</sup>Department of Chemical Engineering, Puducherry Technological University, Puducherry 605014, India. ✉email: seyedali.sajadian@gmail.com; chandrasekhar@ptuniv.edu.in

T	System temperature (K)
$y_2$	Drug solute solubility in mole fraction

### Greek symbols

$\hat{\phi}$	Fugacity coefficient
$\beta, \gamma, \Delta\delta$	Eq. (26) Constants
$\rho_1$	Solvent density
$\kappa, \kappa', \kappa''$	Association numbers

Diabetes mellitus is a common metabolic disorder in which blood glucose levels are too high during a long period of time, which is increasing rapidly over the world and being considered one of the main threats to public health in the twenty-first century. It is predicted that by 2030, 366 million people worldwide will be affected by diabetes, of which 90% will be type II of this disease<sup>1</sup>. The conventional diabetes treatment is associated with some side effects such as weight gain, hypoglycemia, digestive problems, and gastric intolerance. For these reasons, extensive research has been conducted to find novel drug delivery systems for this disease.

Sitagliptin phosphate, a dipeptidyl peptidase-4 (DPP-4) inhibitor, is one of the most effective anti-hyperglycemic agents which has been included in the list of diabetes drugs since 2006 with the FDA approval<sup>2</sup>. The use of sitagliptin phosphate effectively reduces the fasting glucose and glycosylated hemoglobin A1C (HbA1c) levels in type II diabetic patients<sup>3</sup>. However, the biological half life of this drug is short (about 3.6 h in rats), and it is eliminated quickly, implying the use of a high daily dose (prescribed as two doses of 50 mg day<sup>-1</sup>), which is not favorable for patients. This problem can be solved using an efficient drug delivery system with a prolonged and controlled release rate and increased adsorption efficiency of the drug<sup>2,4,5</sup>.

It has been reported that nano-sized drug delivery systems can deliver the required concentration of the drug to the target site of the body in a reasonable time and, as a result, increase the drug bioavailability and decrease its dosage and side effects<sup>6</sup>. Nanoparticles and the various types of polymeric nano formulations are the most common drug delivery systems which have shown satisfactory results in this regard. However, the method of producing these systems significantly influences their characteristics and, thus, their therapeutic efficacy. The conventional methods of producing drug delivery systems have some disadvantages, including non-uniformity of the size and morphology of the obtained particles, the consumption of a lot of organic solvent and subsequently the need for several purification steps to remove residual solvents and to reach pharmaceutical standards, involving the damage of the pharmaceutical compound due to severe operational conditions<sup>7</sup>. Therefore, the design and development of novel techniques to produce efficient drug delivery systems is one of the most attractive research areas.

It has been shown that the scCO<sub>2</sub>-based methods can satisfactorily replace the conventional methods used to produce various pharmaceutical formulations. The FDA's approval for the use of CO<sub>2</sub> as a permitted solvent in the pharmaceutical industry, as well as its unique characteristics, such as abundance, low cost, environmentally friendly nature, and recyclability, are the most important positive features of CO<sub>2</sub><sup>7</sup>, which have its use in the pharmaceutical industries. Different techniques based on supercritical have been developed to produce nano-sized drugs, like supercritical antisolvent (SAS)<sup>8</sup>, supercritical solvent impregnation (SSI)<sup>9</sup>, rapid expansion of a supercritical solution (RESS)<sup>10</sup>, and some others<sup>11–15</sup>.

The solubility of the desired medicine in scCO<sub>2</sub> is an important factor that should be known to select the appropriate supercritical fluid-based method for drug designing. For this reason, determining the solubility of different drugs in scCO<sub>2</sub> has become a relevant research topic in recent years. Moreover, the theoretical determination of the solubility of drugs in scCO<sub>2</sub> has attracted much attention due to the complexity and high cost of the experimental process. The empirical models, thermodynamic models based on various equations of state, intelligence models (e.g., artificial neural networks), molecular modeling and machine learning models are the common models used for this purpose. The empirical models and the equations of state-based models are the most widely used ones. The empirical models, also known as density-based models, are the simplest theoretical models that have been used to correlate the experimental solubility data of solutes in scCO<sub>2</sub> since 1978<sup>16</sup>. These models allow to calculate with acceptable accuracy the solubility of a solute based on the density of the supercritical solvent (scCO<sub>2</sub>) at the desired temperature and pressure, without the need of the thermodynamic and chemical properties of the solute. The use of these models to predict the supercritical solubility of various drugs has been confirmed by many researchers<sup>17–21</sup>.

In this study, the solubility of sitagliptin phosphate in scCO<sub>2</sub> was measured at temperatures of 308, 318, 328, and 338 K, and at pressures of 12–30 MPa. In addition, the solubility of the drug was theoretically determined using some well-known empirical models and a new association model.

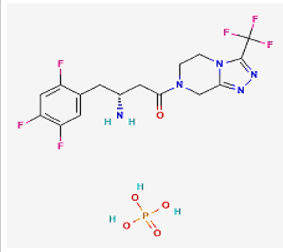

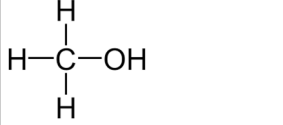
## Experimental

### Materials used

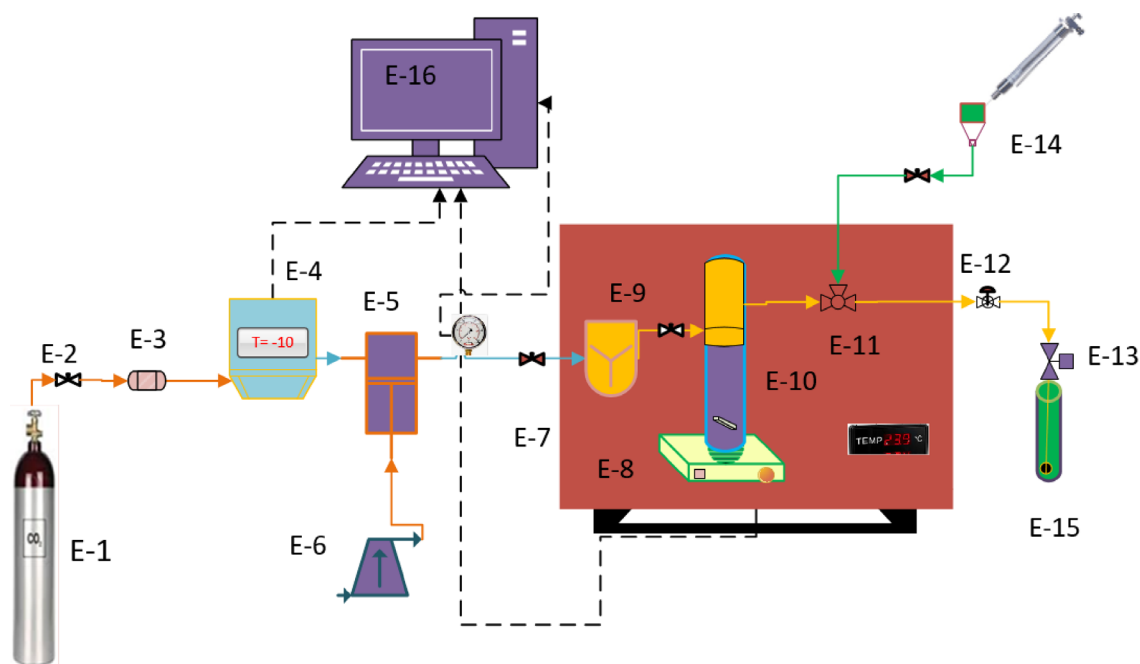
The physicochemical properties of *sitagliptin phosphate* and the other chemicals that were utilized in the study can be found in Table 1. This includes the chemical's structure as well as its molar mass ( $M_w$ ), formula, purity, and CAS number. These substances did not require any further processing of any kind before their use.

### Experimental section

The Fig. 1 shows the apparatus used for the measurement of the Sitagliptin solubility in scCO<sub>2</sub>. More details about this system can be found in our previous studies<sup>22–24</sup>. This laboratory setup includes a CO<sub>2</sub> tank, a cooling unit, a high-pressure pump, an equilibrium cell and a magnetic stirrer, which are clearly marked in the Fig. 1.

Compound	Structure	MW (g mol <sup>-1</sup> )	$\lambda_{\max}$ (nm)	CAS number	Minimum purity	Manufacture
Sitagliptin phosphate		407.31	268	654671-78-0	99% (m/m)	Amin Pharmaceutical Company (Iran) (Esfahan, Iran)
Carbon dioxide		44.01		124-38-9	99.99% (GC)	Aboughadare Co. (Shiraz, Iran)
Methanol		32.04		67-68-5	99% (GC)	Merck Group (Darmstadt, Germany)

**Table 1.** The molecular structure and physicochemical properties of the materials examined in this study.



Displayed Text	Description	Displayed Text	Description
<b>E1</b>	CO <sub>2</sub> Cylinder	<b>E9</b>	Coil
<b>E2</b>	Needle Valve	<b>E10</b>	Cell
<b>E3</b>	Filter	<b>E11</b>	Three -port
<b>E4</b>	Refrigerator Unit	<b>E12</b>	Back pressure
<b>E5</b>	High Pressure Pump	<b>E13</b>	Metering valve
<b>E6</b>	Air compressor	<b>E14</b>	Syringe
<b>E7</b>	Oven	<b>E15</b>	Collection Vial
<b>E8</b>	Magnetic stirrer	<b>E16</b>	Panel

**Figure 1.** Schematic diagram of solubility device.

In this solubility measurement method, initially, CO<sub>2</sub> from the tank at 60 bar, after passing through the molecular sieve filter (1 μm pores) and removing pollution, entered the refrigerator unit for its liquefaction by decreasing temperature from ambient to about -20 °C. Then liquid CO<sub>2</sub> was pressurized using a high-pressure pump until reached the appropriate pressure. The pressure values were controlled and recorded on both the pressure gauge (WIKA, Germany) and pressure transmitter with an accuracy of  $u(P) = 0.1$  MPa. After adjusting the pressure, the liquefied CO<sub>2</sub> entered to the equilibrium cell whose volume was 70 mL. In the cell, liquefied CO<sub>2</sub> was contacted with the drug (Sitagliptin phosphate) that was already loaded in the cell.

The equilibrium cell was placed in an oven with temperature control with an accuracy of  $u(T) = \pm 1$  K. Also, a magnet stirrer was used to achieve a complete saturation of the drug in scCO<sub>2</sub>. The time required for the process was 120 min. After equilibrium, using the opening a 2-status 3-way port valve and reducing the pressure, saturated scCO<sub>2</sub> (600 μL) was delivered into the injection loop. Finally, by opening the micrometer valve, saturated scCO<sub>2</sub> was collected into a vial which was already loaded with 4 mL of methanol. Further, the loop was washed with 1 mL of methanol through an external line. During the experiments pressure was controlled with a back pressure valve. Sitagliptin absorbance in methanol was measured with a spectrophotometer- Perkin-Elmer UV-Vis at 268 nm ( $\lambda_{max}$ ) with the calibration curve (with a regression coefficient of 0.998). The experimental runs were performed three times to determine averages. The relationships used to calculate the solubility of Sitagliptin in scCO<sub>2</sub> at different temperatures and pressures, in terms of mole fraction ( $y$ ) and equilibrium solubility ( $S$  (g L<sup>-1</sup>)), are reported in our previous work<sup>25</sup>.

## Results and discussion

### Experimental solubility

The reliability of the solubility device was tested by determining the solubility of naphthalene at a temperature of 308 K and different pressure values was measured by the used setup used in the work and the obtained data was compared with reported data by Iwai et al.<sup>26</sup>, Yamini et al.<sup>27</sup> and Sodeifian et al.<sup>28</sup>. These data are listed in Table 2.

The solubility data for (R)-4-oxo-4-[3-(trifluoromethyl)-5,6-dihydro [1,2,4] triazolo[4,3-a] pyrazin-7(8H)-yl]-1-(2,4,5-trifluorophenyl) butan-2-amine (also known as *sitagliptin phosphate*) in scCO<sub>2</sub> at different temperature (308, 318, 328 and 338 K) and pressure (12 and 30 MPa) values are shown in Table 3. Crossover points in Fig. 2 are observed for different isotherms between 15 and 16.5 MPa. Below the crossover point's solubility increase is influenced due to increase in the density of scCO<sub>2</sub>, on the other hand above the crossover points the increase in solubility influenced by increase in sublimation pressure of the solute.

From Fig. 2, for an isotherm higher solubility is observed at higher pressures and it is due to enhancement of scCO<sub>2</sub> density at higher pressures. The effect of temperature on solubility is typical in nature and crossover points are observed. Below the crossover point's density of scCO<sub>2</sub> influence the solubility, when density of scCO<sub>2</sub> is higher correspondingly solubility is high even though temperature is lower. On the other hand above the crossover point's solubility increases with temperature and it is due to increase in sublimation pressure of the solute. Thus, temperature has dual effect on solubility via solvent density and solute sublimation pressure.

### Modeling

Solubility of drugs in supercritical fluids was modeled using different approaches that can be classified in density, equations of state, solid-liquid equilibrium and intelligence-based models. However, each approach has its own advantages and drawbacks. The density-based models are simple and easy to apply for data correlation due to doesn't require solute information such as critical properties, acentric factor and sublimation pressure. *Sitagliptin phosphate* is a typical compound, and its acentric factor, critical properties (T<sub>c</sub> and P<sub>c</sub>) molar volumes and sublimation pressures can't be predicted using regular group contribution methods<sup>29-32</sup>, due to the presence of phosphate in its chemical structure. Therefore, equation of state (EOS) and solid-liquid equilibrium methods cannot be applied to correlate the solubility data of sitagliptin phosphate. Thus, only semi-empirical models (*i.e.*, density-based model) are useful in data correlation. In this work for data correlation Josef Chrastil model<sup>33</sup>, Reformulated Chrastil model<sup>34</sup>, Méndez-Santiago and Teja (MST) model<sup>35</sup>, Bartle et al. model<sup>36</sup> and Kumar and Johnston (KJ) model<sup>37</sup> were used. For a better data correlation, a new association model requiring only density, pressure, and temperature of scCO<sub>2</sub> was proposed. Following subsections discuss about the models considered in detail.

#### Josef Chrastil model

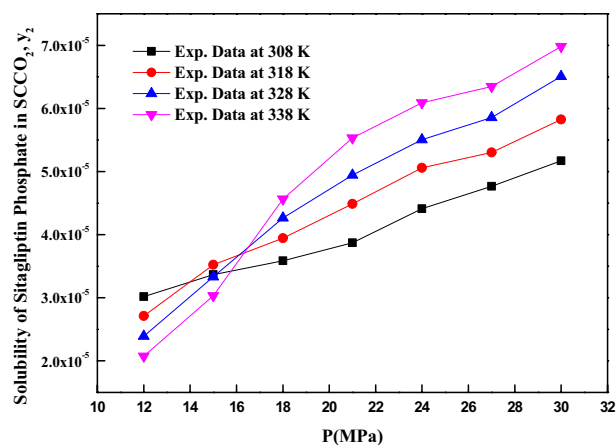
According to this model, the solubility of solutes in SCF is expressed with the following relation:

Pressure (MPa) <sup>a</sup>	Iwai et al. <sup>36</sup> ( $y \times 10^3$ )	Yamini et al. <sup>37</sup> ( $y \times 10^3$ )	Sodeifian et al. <sup>38</sup> ( $y \times 10^3$ )	This work ( $y \times 10^3$ ) <sup>a</sup>
10.7	–	11.6	11.4	11.7 ± 0.2
13.8	14.1	15.2	14.3	14.8 ± 0.3
16.8	16.5	16.2	16.6	16.1 ± 0.3
20.4	17.6	17.4	17.7	17.9 ± 0.2
24.0	–	–	–	19.9 ± 0.4

**Table 2.** Experimental solubility data of naphthalene in sc-CO<sub>2</sub> at 308 K and comparison with the literature data. <sup>a</sup>Standard uncertainty  $u$  are  $u(P) = 0.1$  MPa and relative uncertainty ( $u_r$ ),  $u(y) = 0.10$ .

Temperature <sup>a</sup> (K)	Pressure <sup>a</sup> (MPa)	Density <sup>b</sup> (kg m <sup>-3</sup> )	$\gamma \times 10^4$ (mole fraction)	Standard deviation $\times (10^5)$	Expanded uncertainty of mole fraction ( $10^4$ U)	S (Solubility (g l <sup>-1</sup> ))
308	12	768.42	0.302	0.040	0.101	0.267
	15	816.06	0.337	0.056	0.131	0.316
	18	848.87	0.359	0.072	0.162	0.350
	21	874.4	0.387	0.090	0.197	0.389
	24	895.54	0.441	0.118	0.253	0.454
	27	913.69	0.477	0.154	0.323	0.500
	30	929.68	0.517	0.172	0.360	0.552
318	12	659.73	0.271	0.036	0.091	0.206
	15	743.17	0.352	0.059	0.138	0.301
	18	790.18	0.395	0.079	0.177	0.358
	21	823.7	0.449	0.145	0.304	0.424
	24	850.1	0.506	0.067	0.169	0.494
	27	872.04	0.530	0.100	0.227	0.531
	30	890.92	0.583	0.117	0.263	0.596
328	12	506.85	0.239	0.056	0.122	0.139
	15	654.94	0.333	0.070	0.156	0.250
	18	724.13	0.426	0.085	0.191	0.355
	21	768.74	0.494	0.137	0.292	0.436
	24	801.92	0.551	0.147	0.315	0.507
	27	828.51	0.586	0.176	0.372	0.557
	30	850.83	0.651	0.217	0.454	0.636
338	12	384.17	0.207	0.028	0.070	0.092
	15	555.23	0.303	0.051	0.119	0.193
	18	651.18	0.456	0.091	0.205	0.341
	21	709.69	0.553	0.074	0.186	0.451
	24	751.17	0.609	0.102	0.239	0.525
	27	783.29	0.635	0.127	0.285	0.571
	30	809.58	0.698	0.163	0.356	0.649

**Table 3.** The experimental data of sitagliptin phosphate solubility in SC-CO<sub>2</sub> based on distinct conditions (temperatures (T) and pressures (P) for binary system). <sup>a</sup>Standard uncertainty  $u$  are  $u(T) = \pm 0.1$  K;  $u(p) = \pm 1$  bar. Also, relative standard uncertainties are obtained below 5% for mole fractions and solubilities. The value of the coverage factor  $k=2$  was chosen on the basis of the level of confidence of approximately 95 percent. <sup>b</sup>Data from the Span–Wagner equation of state<sup>62</sup>.



**Figure 2.** Sitagliptin phosphate solubility vs. pressure.

$$c/\text{kg} \cdot \text{m}^{-3} = (\rho_1/\text{kg} \cdot \text{m}^{-3})^\kappa \exp\left(A_1 + B_1/T/K\right) \quad (1)$$

where  $\kappa$ ,  $A_1$  and  $B_1$  are model constants.

Equation (1) can be rearranged to mole fraction as follows<sup>38</sup>

$$\frac{c/\text{kg} \cdot \text{m}^{-3}}{\rho_1/\text{kg} \cdot \text{m}^{-3}} \frac{M_{\text{ScF}}}{M_{\text{Solute}}} = \frac{M_{\text{ScF}}}{M_{\text{Solute}}} (\rho_1/\text{kg} \cdot \text{m}^{-3})^{\kappa-1} \exp\left(A_1 + B_1/T/K\right) \quad (2)$$

$$\text{mole ratio} = \frac{c/\text{kgmol} \cdot \text{m}^{-3}}{\rho_1/\text{kgmol} \cdot \text{m}^{-3}} = \frac{M_{\text{ScF}}}{M_{\text{Solute}}} (\rho_1/\text{kg} \cdot \text{m}^{-3})^{\kappa-1} \exp\left(A_1 + B_1/T/K\right) \quad (3)$$

Mole fraction ( $y_2$ ) and mole ratio are related as follows

$$\frac{c/\text{kgmol} \cdot \text{m}^{-3}}{\rho_1/\text{kgmol} \cdot \text{m}^{-3}} = \frac{y_2/\text{mole fraction}}{1 - y_2/\text{mole fraction}} \quad (4)$$

$$y_2/\text{mole fraction} = \frac{c/\text{kgmol} \cdot \text{m}^{-3}}{\rho_1/\text{kgmol} \cdot \text{m}^{-3}} \left/ \left[ 1 + \frac{c/\text{kgmol} \cdot \text{m}^{-3}}{\rho_1/\text{kgmol} \cdot \text{m}^{-3}} \right] \right. \quad (5)$$

$$y_2/\text{mole fraction} = \frac{M_{\text{ScF}}}{M_{\text{Solute}}} (\rho_1/\text{kg} \cdot \text{m}^{-3})^{\kappa-1} \exp\left(A_1 + B_1/T/K\right) \left/ \left[ 1 + \frac{M_{\text{ScF}}}{M_{\text{Solute}}} (\rho_1/\text{kg} \cdot \text{m}^{-3})^{\kappa-1} \exp\left(A_1 + B_1/T/K\right) \right] \right. \quad (6)$$

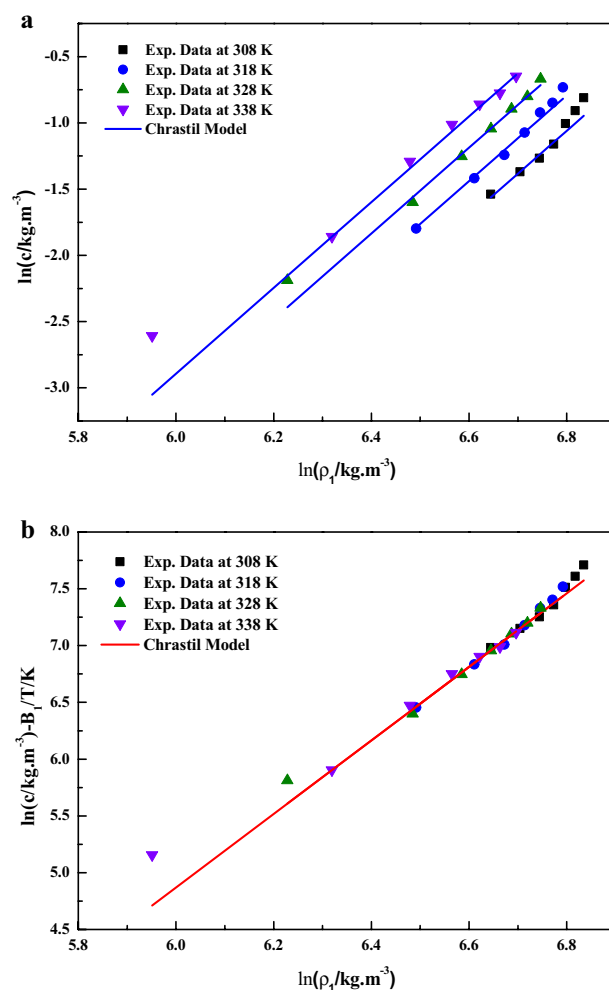
In Eq. (6), the model constants are treated as independent of temperature and their values are obtained by regression with experimental data<sup>38</sup>. The obtained values are reported in Table 4. It is quite evident that a linear plot is observed when the data is depicted as  $\ln(c/\text{kg} \cdot \text{m}^{-3})$  vs.  $\ln(\rho_1/\text{kg} \cdot \text{m}^{-3})$  (Fig. 3a) and as  $\ln(c/\text{kg} \cdot \text{m}^{-3}) - B_1/T/K$  vs.  $\ln(\rho_1/\text{kg} \cdot \text{m}^{-3})$  (Fig. 3b), this confirms the applicability of the Chrastil model to the solubility data<sup>39</sup>. From the constant  $B_1$ , total heat of reaction is calculated (i.e.,  $\Delta H_{\text{Total}} = B_1R$ ), the obtained values are reported in Table 5

#### Reformulated Chrastil model

According to this model, solubility is a function of  $\kappa'$  (association number),  $\rho_1$  (solvent density (scCO<sub>2</sub>)) and T (temperature). In Eq. (7), it is important to note that depending on the reference fugacity units, R units are selected.

Sl. no	Name of the model & Equation number	Model parameters	R <sup>2</sup>	R <sup>2</sup> <sub>adj</sub>	AARD%
1	Chrastil Model & Eq. (6)	$\kappa = 3.2364$ ; $A_1 = -14.548$ ; $B_1 = -2624.0$	0.92249	0.91951	4.97
2	Reformulated Chrastil Model & Eq. (7)	$\kappa' = 3.2439$ ; $A_2 = -17.896$ ; $B_2 = -1910.2$	0.96697	0.96570	4.95
3	MT Model & Eq. (8)	$A_3 = -6486.6$ ; $B_3 = 2.193$ ; $C_3 = 10.103$	0.91635	0.9059	8.721
4	Bartle et. al. Model & Eq. (9)	$A_4 = 9.8241$ ; $B_4 = -4861.2$ ; $C_4 = 0.0065735$	0.89618	0.89219	9.06
5	KJ Model & Eq. (10)	$A_5 = -4.197$ ; $B_5 = 0.0031559$ ; $C_5 = -2671.2$	0.98536	0.98480	3.16
6	New Association Model & Eq. (30)	$\kappa'' = 1.1945$ ; $A_6 = -1519.5$ ; $B_6 = 2.1846$ ; $C_6 = 0.0024843$ ; $D_6 = -20.894$	0.98817	0.98772	2.53

**Table 4.** The correlation results of the sitagliptin phosphate–CO<sub>2</sub> system provided by semi-empirical models and new association model.



**Figure 3.** (a) Experimental data of supercritical solubility of sitagliptin phosphate (points) compared to data calculated with the Chrastil model (line). (b) Results of self-consistency analysis for the Chrastil model.

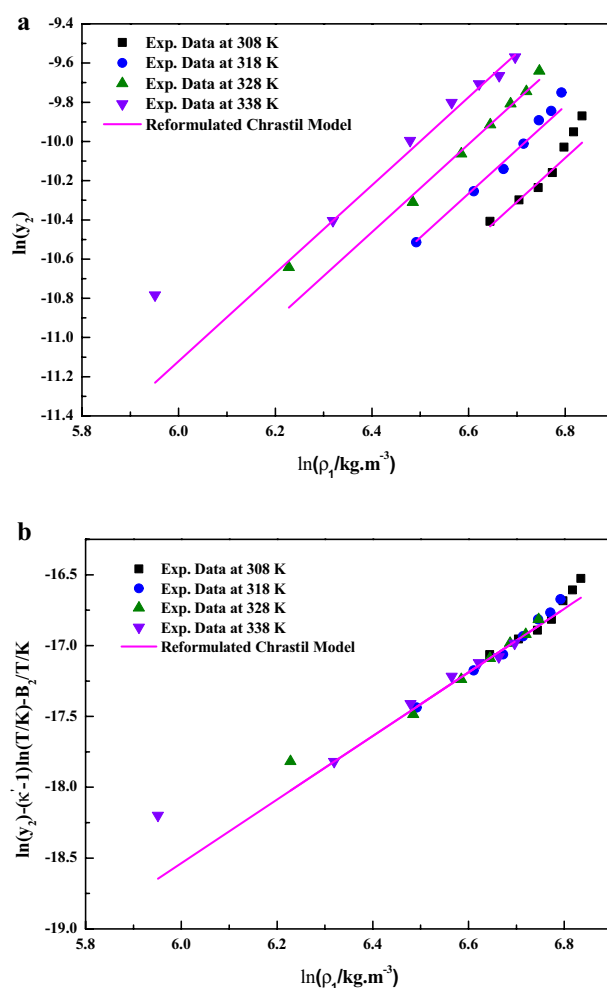
Model	Property		
	Total enthalpy in $\text{kJ mol}^{-1}$	Sublimation enthalpy, $\text{kJ mol}^{-1}$	Solvation enthalpy, $\text{kJ mol}^{-1}$
Chrastil Model <sup>a</sup>	21.815 <sup>a</sup>		*- 18.601 <sup>b</sup>
Reformulated Chrastil Model <sup>c</sup>	15.881 <sup>c</sup>		** - 24.535 <sup>d</sup>
Bartle et al. Model <sup>e</sup>		40.416 <sup>e</sup>	

**Table 5.** Calculated enthalpies of sitagliptin phosphate–CO<sub>2</sub> system provided by semi-empirical models. \*Solvation enthalpy<sup>b</sup> = Total Enthalpy obtained from Chrastil Model<sup>a</sup>–Sublimation Enthalpy obtained from Bartle et al. Model<sup>e</sup>; \*\*Solvation enthalpy<sup>d</sup> = Total Enthalpy obtained from reformulated Chrastil Model<sup>c</sup>–Sublimation Enthalpy obtained from Bartle et al. Model<sup>e</sup>; A negative sign is attributed solvation enthalpy.

$$y_2 / \text{mole fraction} = \left( \frac{R / \text{atm} \cdot \text{m}^3 \cdot \text{kgmol}^{-1} K^{-1} T / K \rho_1 / \text{kg} \cdot \text{m}^{-3}}{M_{ScF} / \text{kg} \cdot \text{kgmol}^{-1} \cdot f^* / 1 \text{atm}} \right)^{\kappa'-1} \exp \left( A_2 + \frac{B_2}{T/K} \right) \quad (7)$$

where R denotes universal gas constant ( $0.082057 \text{ atm m}^3 \text{ kgmol}^{-1} \text{ K}^{-1}$ ),  $M_{ScF}$  is molecular weight of solvent (For CO<sub>2</sub>  $44.01 \text{ kgmol}^{-1}$ ),  $f^*$  is reference fugacity (1 atm) and  $A_2$  and  $B_2$  are the reformulated model constants.

In Eq. (7), the model constants were treated as independent of temperature and their values were obtained by regression with experimental data. The obtained values are reported in Table 4. It is quite evident that a linear plot is observed when the data are depicted as  $\ln(y_2)$  vs.  $\ln(\rho_1 / \text{kg} \cdot \text{m}^{-3})$  (Fig. 4a) and as  $\ln(y_2) - (\kappa' - 1) \ln(T) - B_2/T/K$  vs.  $\ln(\rho_1 / \text{kg} \cdot \text{m}^{-3})$  (Fig. 4b), this confirms the applicability of the



**Figure 4.** (a) Experimental data of supercritical solubility of sitagliptin phosphate (points) compared to data calculated with the Reformulated Chrastil Model (line). (b) Results of self-consistency analysis for the Reformulated Chrastil Model.

reformulated Chrastil model to the solubility data. From the constant  $B_2$ , total heat of reaction is calculated (i.e.,  $\Delta H_{Total} = B_2R$ ), the obtained values are reported in Table 5.

#### Méndez-Santiago and Teja (MT) model

Internal consistency of the measured solubility data was checked with this model. It is stated as Eq. (8) and when  $T \ln(y_2P) - C_3T$  vs.  $\rho_1$  is established, all data points fall around a single straight line.

$$T/K \cdot \ln(y_2P/\text{bar}) = A_3 + B_3 \cdot \rho_1/\text{kg} \cdot \text{m}^{-3} + C_3 \cdot T/K \quad (8)$$

where  $A_3$  to  $C_3$  are the model constants.

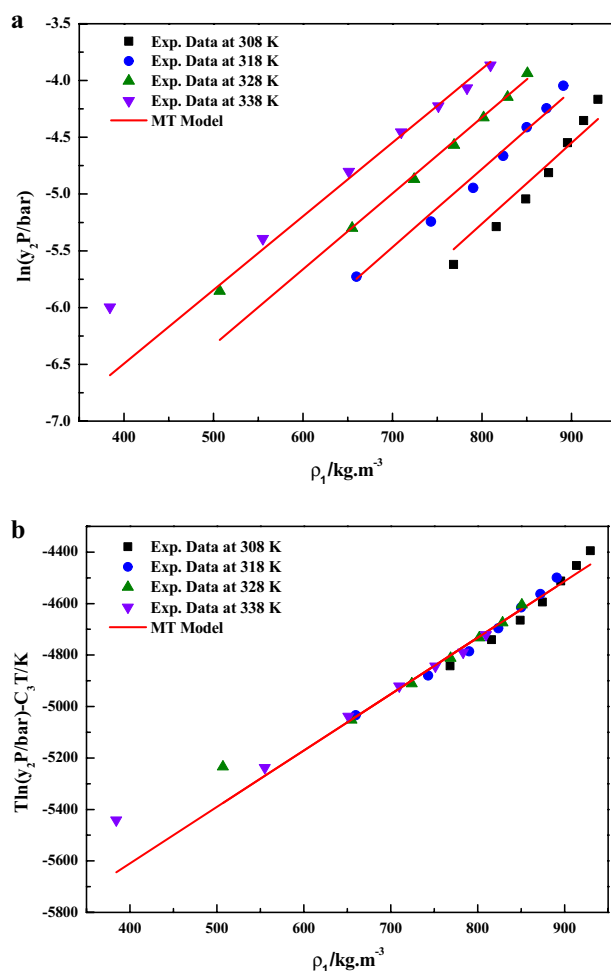
In Eq. (8), the model constants were treated as independent of temperature and their values were obtained by regression with experimental data. The obtained values were reported in Table 4. The experimental data obtained in this work is checked for consistency with the help of Mendez-Santiago and Teja model (MT model). According to the MT model, the solubility data at different temperatures collapsed into a single line. It is quite evident that linear plots are observed when the data are depicted as  $\ln(y_2 \cdot P/\text{bar})$  vs.  $\rho_1/\text{kg} \cdot \text{m}^{-3}$  (Fig. 5a) and as  $T/K \ln(y_2 \cdot P/\text{bar}) - C_3T/K$  vs.  $\rho_1/\text{kg} \cdot \text{m}^{-3}$  (Fig. 5b), this confirms the applicability of the MT model to the solubility data.

#### Bartle et al., model

According to the model the solubility was expressed as Eq. (9)

$$\ln\left(\frac{y_2 \cdot P}{P_{ref}}\right) = A_4 + \frac{B_4}{T/K} + C_4(\rho_1/\text{kg} \cdot \text{m}^{-3} - \rho_{ref}/\text{kg} \cdot \text{m}^{-3}) \quad (9)$$





**Figure 5.** (a) Experimental data of supercritical solubility of sitagliptin phosphate (points) compared to data calculated with the MT Model (line). (b) Results of self-consistency analysis for the MT Model.

where reference pressure is 0.1 MPa or 1 bar, reference density is  $700 \text{ kg m}^{-3}$  and  $A_4$  to  $C_4$  are the model constants. From the constant  $B_4$ , sublimation enthalpy is calculated (i.e.,  $\Delta_{\text{sub}}H = -B_4R$ ).

In Eq. (9), the model constants were treated as independent of temperature and their values were obtained by regression with experimental data. The obtained values were reported in Table 4 it is quite evident that linear plots are observed when the data are depicted as  $\ln\left(\frac{y_2 P}{P_{\text{ref}}}\right)$  vs.  $(\rho_1 - \rho_{\text{ref}})/\text{kg}\cdot\text{m}^{-3}$  (Fig. 6a) and as  $\ln\left(\frac{y_2 P}{P_{\text{ref}}}\right) - \frac{B_4}{T/K}$  vs.  $(\rho_1 - \rho_{\text{ref}})/\text{kg}\cdot\text{m}^{-3}$  (Fig. 6b) this confirms the applicability of the Bartle et al. model to the solubility data.

#### Kumar and Johnston (KJ) model

According to the model the solubility was expressed as Eq. (10)

$$\ln(y_2) = A_5 + B_5(\rho_1/\text{kg}\cdot\text{m}^{-3}) + \frac{C_5}{T/K} \quad (10)$$

where  $A_5$  to  $C_5$  are the model constants.

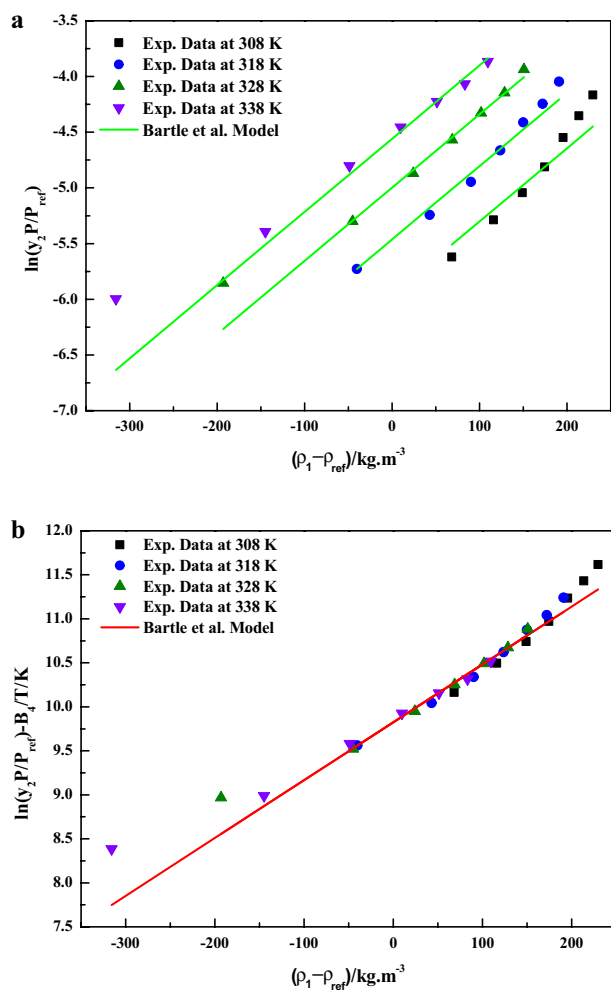
In Eq. (10), the model constants were treated as independent of temperature and their values were obtained by regression with experimental data. The obtained values were reported in Table 3 it is quite evident that a linear plots are observed when the data are depicted as  $\ln(y_2) - \frac{C_5}{T/K}$  vs.  $\rho_1/\text{kg}\cdot\text{m}^{-3}$  (Fig. 7a) and as  $\ln(y_2) - \frac{C_5}{T/K}$  vs.  $\rho_1/\text{kg}\cdot\text{m}^{-3}$  (Fig. 7b), this confirms the applicability of the KJ model to the solubility data.

#### New association model

If one molecule of a solute (A) associates with  $\kappa''$  molecules of solvent (B) to form one molecule of a solvato complex  $AB_{\kappa}$  in equilibrium with the gaseous system<sup>33</sup>,



Equation (12) represents the equilibrium constant in terms of the individual component's fugacity



**Figure 6.** (a) Experimental data of supercritical solubility of sitagliptin phosphate (points) compared to data calculated with the Bartle et al. Model (line). (b) Results of self-consistency analysis for the Bartle et al. Model.

$$K_f = \frac{\left(\hat{f}_{AB_\kappa} / f_{AB_\kappa}^*\right)_{ScP}}{\left(\frac{\hat{f}_A}{f_A^*}\right)_S \left(\left(\frac{\hat{f}_B}{f_B^*}\right)^{\kappa''}\right)_{ScP}} \quad (12)$$

where ScP represents the supercritical phase, S represents the solute phase and  $f^*$  is reference fugacity. The fugacity for each component can be calculated by the following equations<sup>40–42</sup>.

$$\hat{f}_A = \gamma_A \hat{\phi}_A P \quad (13)$$

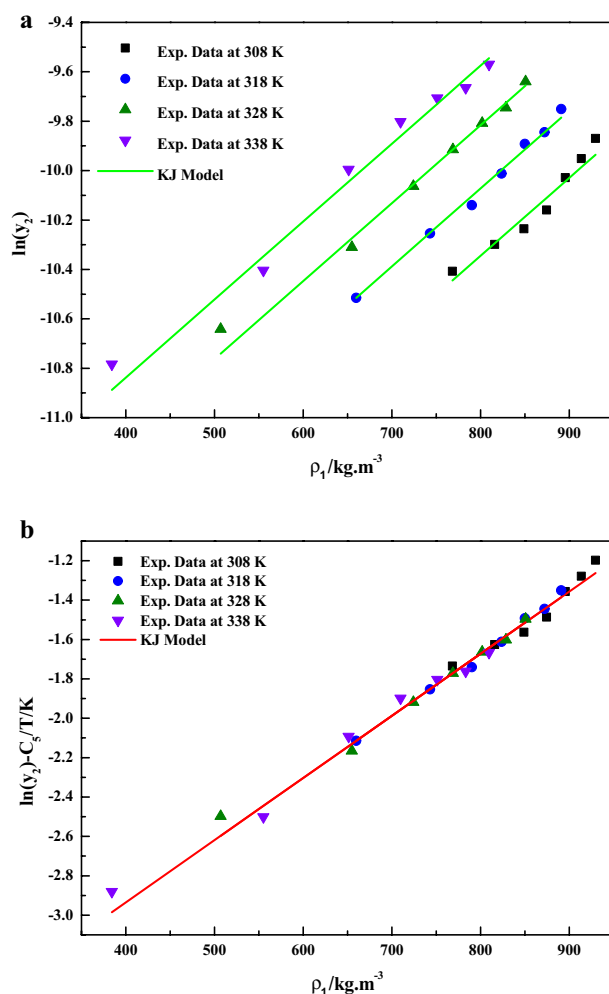
$$\hat{f}_B = \gamma_B \hat{\phi}_B P \quad (14)$$

$$\hat{f}_{AB_\kappa} = \gamma_{AB_\kappa} \hat{\phi}_{AB_\kappa} P \quad (15)$$

$$f_{AB_\kappa}^* = \phi_{AB_\kappa}^* P^* \quad (16)$$

$$f_A^* = \phi_A^* P^* \quad (17)$$

$$f_B^* = \phi_B^* P^* \quad (18)$$



**Figure 7.** (a) Experimental data of supercritical solubility of sitagliptin phosphate (points) compared to data calculated with the KJ Model (line). (b) Results of self-consistency analysis for the KJ Model.

Here the main assumption is fluid-phase component does not dissolve in the solid. i.e., the solid is pure. Solute A exists in an associated state in ScP

$$y_B + y_{AB_k} = 1 \quad (19)$$

where  $y_B, y_{AB_k}$  are mole fraction of solvent and solvato complex respectively.

Since the solute A mainly exists in an associating state, the solubility of solute A in ScP is<sup>43–45</sup>

$$y_2 = \frac{y_{AB_k}}{1 + \kappa'' y_{AB_k}} \quad (20)$$

when standard state of the solute A is treated as pure solute at system pressure (P) and temperature (T), then

$$\hat{f}_A = f_A \quad (21)$$

The fugacity of pure solute can be written as

$$f_A = P_A^{sub} \exp\left(\frac{V_A(P - P_A^{sub})}{RT}\right) \quad (22)$$

where  $P_A^{sub}$  is the sublimation pressure of the pure solid, and  $V_A$  is the molar volume of the pure solid at system temperature (T), and pressure, (P).

Substituting Eqs. (13)–(18) and Eq. (22) in Eq. (12) gives Eq. (23)

$$K_f = \frac{\left( \frac{y_{AB_k} \hat{\phi}_{AB_k} P}{\phi_{AB_k}^* P^*} \right)}{\left( \frac{P_A^{sub} \exp\left(\frac{V_A(P - P_A^{sub})}{RT}\right)}{\phi_A^* P^*} \right) \left( \frac{y_B \hat{\phi}_B P}{\phi_B^* P^*} \right)^{\kappa''}} \quad (23)$$

$$\begin{aligned} \ln(K_f) = & \ln(y_{AB_k}) + \ln\left(\frac{\hat{\phi}_{AB_k}}{\phi_{AB_k}^*}\right) + \ln(P/P^*) + \ln(\phi_A^*) - \ln(P_A^{sub}/P^*) - \frac{V_A(P - P_A^{sub})}{RT} \\ & - \kappa'' \ln(y_B) - \kappa'' \ln\left(\frac{\hat{\phi}_B}{\phi_B^*}\right) - \kappa'' \ln(P/P^*) \end{aligned} \quad (24)$$

The equilibrium constant,  $K_f$ , may be expressed as  $\ln(K_f) = \frac{\Delta H_s}{RT} + q_s$ , where  $\Delta H_s$ , the heat of solvation and  $q_s$  is a constant and  $V_A P / RT$  may be expressed as  $ZV_A \rho / M$  where  $\rho$  is the density of the supercritical phase. At the supercritical state,  $\rho$  is a function of three variables namely pressure, temperature and composition. Thus, the fugacities in Eq. (24) are a very complex function of pressure, temperature and composition.

Then Eq. (24) may be expressed as

$$\begin{aligned} \ln(y_{AB_k}) - \kappa'' \ln(y_B) + (1 - \kappa'') \ln(P/P^*) = & -\ln\left(\frac{\hat{\phi}_{AB_k}}{\phi_{AB_k}^*}\right) - \ln(\phi_A^*) + \ln(P_A^{sub}) - \ln(P^*) \\ & + \frac{ZV_A \rho}{M} - \frac{V_A P^{sub}}{RT} + \kappa'' \ln\left(\frac{\hat{\phi}_B}{\phi_B^*}\right) + \frac{\Delta H_s}{RT} + q_s \end{aligned} \quad (25)$$

The sublimation pressure of the solid solute may be expressed as

$$R \ln(P_A^{sub}) = \beta + \frac{\gamma}{T} + \Delta_{sub} \delta \ln\left(\frac{T}{298.15}\right) \quad (26)$$

where  $\beta$ ,  $\gamma$  and  $\Delta_{sub} \delta$  are temperature independent parameters.

When  $\frac{V_A P^{sub}}{RT}$  ( $\sim 10^{-9}$ ) term is neglected (since the sublimation pressures ( $\sim 10^{-4}$ ) and molar volume of solid solutes ( $\sim 10^{-4}$ ) are very low) and density of solution is treated as approximately as density of supercritical fluid

$$\ln(y_{AB_k}) - \kappa'' \ln(y_B) + (1 - \kappa'') \ln(P/P^*) = \frac{A_6}{T} + B_6 \ln(T) + C_6 \rho_1 + D_6 \quad (27)$$

where  $A_6 = \frac{\Delta H_s}{R} + \frac{\gamma}{R}$ ,  $B_6 = \Delta_{sub} \delta / R$ ,  $C_6 = \frac{ZV_A}{M}$  and  $D_6 = -\ln\left(\frac{(\phi_A^*) \left(\frac{\hat{\phi}_{AB_k}}{\phi_{AB_k}^*}\right)}{\left(\frac{\hat{\phi}_B}{\phi_B^*}\right)^{\kappa''}}\right) - \ln P^*$   
 $+ q_s + \frac{\beta}{R} - \frac{\Delta_{sub} \delta \ln(298.15)}{R}$

Equation (27) may be written as Eq. (28)

$$y_{AB_k} = (y_B)^{\kappa''} \left(\frac{P}{P^*}\right)^{(\kappa''-1)} \exp\left(\frac{A_6}{T} + B_6 \ln(T) + C_6 \rho_1 + D_6\right) \quad (28)$$

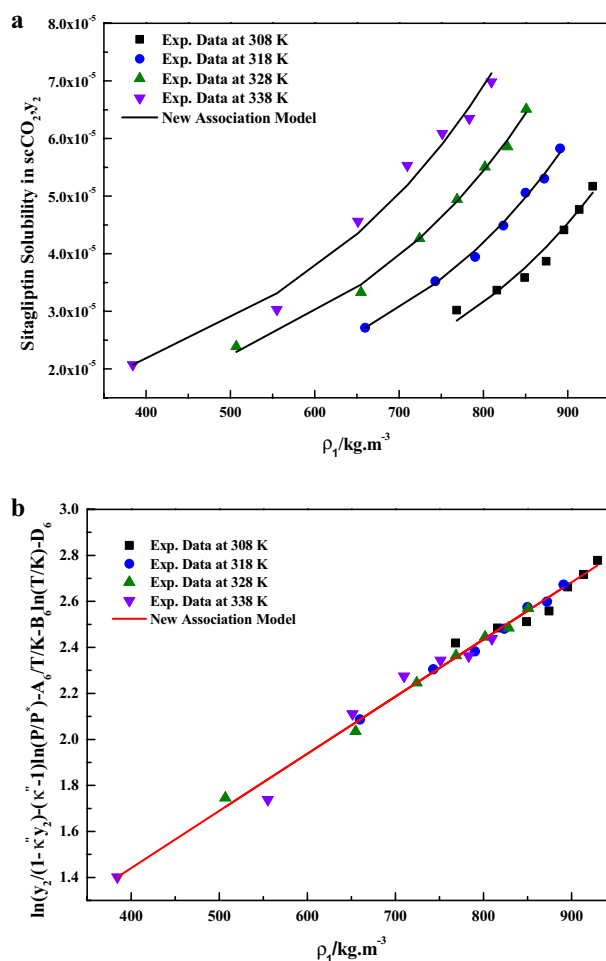
Because the solubility of drug in scCO<sub>2</sub> are very dilute, therefore for a binary system we may assume  $y_B$  is unity. Then Eq. (28) reduced to Eq. (29)

$$y_{AB_k} = \left(\frac{P}{P^*}\right)^{(\kappa''-1)} \exp\left(\frac{A_6}{T} + B_6 \ln(T) + C_6 \rho_1 + D_6\right) \quad (29)$$

Combining Eq. (20) and Eq. (29) gives expression for solubility Eq. (30)

$$y_2 = \frac{\left(\frac{P}{P^*}\right)^{(\kappa''-1)} \exp\left(\frac{A_6}{T} + B_6 \ln(T) + C_6 \rho_1 + D_6\right)}{1 + \kappa'' \left(\frac{P}{P^*}\right)^{(\kappa''-1)} \exp\left(\frac{A_6}{T} + B_6 \ln(T) + C_6 \rho_1 + D_6\right)} \quad (30)$$

From Eq. (30), it is clear that solubility is a function of density, temperature and association number (i.e.,  $y_2 = y_2(\rho_1, T, \kappa'')$ ) and further all equations are dimensionally consistent. Hereafter, this equation may be called as the new association model. In Eq. (30), the model constants were treated as independent of temperature and their values were obtained by regression with experimental data. The obtained values are reported in Table 4 it is quite evident that a better fit is observed when the data is plotted as Sitagliptin Phosphate solubility,  $y_2$  vs.  $\rho_1 / \text{kg} \cdot \text{m}^{-3}$  (Fig. 8a). It is important to note that Fig. 8a is not linear due to its functionality (i.e.,  $y_2 = y_2(\rho_1, T, \kappa'')$ ). However, a linear plot is observed when the data are depicted as



**Figure 8.** (a) Sitagliptin phosphate solubility,  $y_2$  vs.  $\rho_1/\text{kg} \cdot \text{m}^{-3}$ . (b) Results of self-consistency analysis for the New Association Model.

$\ln(y_2/(1-\kappa''y_2)) - (\kappa''-1)\ln(P/P^*) - A_6/T - B_6\ln(T) - D_6$  vs.  $\rho_1/\text{kg} \cdot \text{m}^{-3}$  (Fig. 8b), which confirms the applicability of the new association model to the solubility data. Solubility of solids substances in  $\text{scCO}_2$  are best understood in terms of solvato-complex formation, thus the interactions between sitagliptin phosphate (solute) and supercritical carbon dioxide (solvent) is visualized as formation of a solvato-complex. The new association model (solvato-complex model) proposed in this study is able to capture solubility phenomena with least AARD% (i.e., 2.53%). Thus, present study confirms solvato-complex theory holds good for this sitagliptin phosphate- $\text{scCO}_2$  system.

## Conclusion

The solubility of (R)-4-oxo-4-[3-(trifluoromethyl)-5,6-dihydro [1,2,4] triazolo[4,3-a] pyrazin-7(8H)-yl]-1-(2,4,5-trifluorophenyl) butan-2-amine (i.e., *sitagliptin phosphate*) was measured by a static method in the pressure range of 12–30 MPa for different temperature values (30, 318, 328 and 338 K). The measured solubilities range from  $(0.2074 \text{ to } 0.698) \times 10^{-4}$  mol fraction of (R)-4-oxo-4-[3-(trifluoromethyl)-5,6-dihydro [1,2,4] triazolo[4,3-a] pyrazin-7(8H)-yl]-1-(2,4,5-trifluorophenyl) butan-2-amine. Further, measured solubilities are reasonably correlated with the Chrastil model, the reformulated Chrastil model, the Méndez-Santiago and Teja (MST) model, the Bartle et al., model, the Kumar and Johnston (KJ) model. The newly proposed association model was able to correlate the solubility data with the lowest absolute relative deviation (2.53%). Calculated sublimation and solvation enthalpies of *Sitagliptin phosphate* in  $\text{scCO}_2$  are  $40.416 \text{ kJ mol}^{-1}$ ,  $-24.535 \text{ kJ mol}^{-1}$  for Bartle et al., model and Bartle et al., model + Chrastil model combination, respectively.

Received: 30 June 2023; Accepted: 12 October 2023

Published online: 16 October 2023

## References

- Sivaprasad, S., Gupta, B., Crosby-Nwaobi, R. & Evans, J. Prevalence of diabetic retinopathy in various ethnic groups: A worldwide perspective. *Surv. Ophthalmol.* **57**, 347–370. <https://doi.org/10.1016/j.survophthal.2012.01.004> (2012).
- Sreeharsha, N. *et al.* Mucoadhesive particles: A novel, prolonged-release nanocarrier of sitagliptin for the treatment of diabetics. *BioMed Res. Int.* **2019**, 3950942. <https://doi.org/10.1155/2019/3950942> (2019).
- Herman, G. A. *et al.* Pharmacokinetics and pharmacodynamic effects of the oral DPP-4 inhibitor sitagliptin in middle-aged obese subjects. *J. Clin. Pharmacol.* **46**, 876–886. <https://doi.org/10.1177/0091270006289850> (2006).
- Kazi, M. *et al.* Development and optimization of sitagliptin and dapagliflozin loaded oral self-nanoemulsifying formulation against type 2 diabetes mellitus. *Drug Deliv.* **28**, 100–114. <https://doi.org/10.1080/10717544.2020.1859001> (2021).
- Haq-Asif, A., Harsha, S., Hodalur-Puttaswamy, N. & Al-Dhubiab, B. An effective delivery system of sitagliptin using optimized mucoadhesive nanoparticles. *Appl. Sci.* **8**, 6 (2018).
- Mukherjee, B. Nanosize drug delivery system. *Curr. Pharmaceut. Biotechnol.* **14**, 1221. <https://doi.org/10.2174/138920101415140804121008> (2013).
- Champeau, M., Thomassin, J. M., Tassaing, T. & Jérôme, C. Drug loading of polymer implants by supercritical CO<sub>2</sub> assisted impregnation: A review. *J. Controll. Release* **209**, 248–259. <https://doi.org/10.1016/j.jconrel.2015.05.002> (2015).
- Prosapio, V., De Marco, I. & Reverchon, E. PVP/corticosteroid microspheres produced by supercritical antisolvent coprecipitation. *Chem. Eng. J.* **292**, 264–275. <https://doi.org/10.1016/j.cej.2016.02.041> (2016).
- Saadati-Ardestani, N. & Amani, M. Supercritical solvent impregnation of sodium valproate nanoparticles on polymers: Characterization and optimization of the operational parameters. *J. CO<sub>2</sub> Utiliz.* **64**, 102159. <https://doi.org/10.1016/j.jcou.2022.102159> (2022).
- Riekes, M. K. *et al.* Enhanced hypotensive effect of nimodipine solid dispersions produced by supercritical CO<sub>2</sub> drying. *Powd. Technol.* **278**, 204–210. <https://doi.org/10.1016/j.powtec.2015.03.029> (2015).
- Jesson, G. *et al.* Carbon dioxide-mediated generation of hybrid nanoparticles for improved bioavailability of protein kinase inhibitors. *Pharm. Res.* **31**, 694–705. <https://doi.org/10.1007/s11095-013-1191-4> (2014).
- Park, J. W. *et al.* A nanosystem for water-insoluble drugs prepared by a new technology, nanoparticulation using a solid lipid and supercritical fluid. *Arch. Pharm. Res.* **36**, 1369–1376. <https://doi.org/10.1007/s12272-013-0187-2> (2013).
- Obaidat, R. M., Tashatoush, B. M., Awad, A. A. & Al-Bustami, R. T. Using supercritical fluid technology (SFT) in preparation of tacrolimus solid dispersions. *AAPS Pharm. Sci. Tech.* **18**, 481–493. <https://doi.org/10.1208/s12249-016-0492-4> (2017).
- Wu, K., Li, J., Wang, W. & Winstead, D. A. Formation and characterization of solid dispersions of piroxicam and polyvinylpyrrolidone using spray drying and precipitation with compressed antisolvent. *J. Pharm. Sci.* **98**, 2422–2431. <https://doi.org/10.1002/jps.21598> (2009).
- Pathak, P., Prasad, G. L., Meziani, M. J., Joudeh, A. A. & Sun, Y.-P. Nanosized paclitaxel particles from supercritical carbon dioxide processing and their biological evaluation. *Langmuir* **23**, 2674–2679. <https://doi.org/10.1021/la062739d> (2007).
- Stahl, E., Schilz, W., Schütz, E. & Willing, E. A quick method for the microanalytical evaluation of the dissolving power of supercritical gases. *Angew. Chem.* **17**, 731–738. <https://doi.org/10.1002/anie.197807311> (1978).
- Shojaee, S., Rajaei, H., Hezave, A., Lashkarbolooki, M. & Esmailzadeh, F. Experimental solubility measurement of cephalixin in supercritical carbon dioxide. *Chem. Ind. Chem. Eng. Q.* **20**, 387–395. <https://doi.org/10.2298/CICEQ121128021S> (2014).
- Zeinolabedini-Hezave, A., Khademi, M. H. & Esmailzadeh, F. Measurement and modeling of mefenamic acid solubility in supercritical carbon dioxide. *Fluid Phase Equilib.* **313**, 140–147. <https://doi.org/10.1016/j.fluid.2011.09.031> (2012).
- Shojaee, S. A., Rajaei, H., Hezave, A. Z., Lashkarbolooki, M. & Esmailzadeh, F. Experimental measurement and correlation for solubility of piroxicam (a non-steroidal anti-inflammatory drugs (NSAIDs)) in supercritical carbon dioxide. *J. Supercrit. Fluids* **80**, 38–43. <https://doi.org/10.1016/j.supflu.2013.03.015> (2013).
- Wang, S.-W., Chang, S.-Y. & Hsieh, C.-M. Measurement and modeling of solubility of gliclazide (hypoglycemic drug) and captopril (antihypertension drug) in supercritical carbon dioxide. *J. Supercrit. Fluids* **174**, 105244. <https://doi.org/10.1016/j.supflu.2021.105244> (2021).
- Arjmand, M., Mirzajanzadeh, M. & Zabihi, F. Measurement and correlation of solid drugs solubility in supercritical systems. *Chin. J. Chem. Eng.* **22**, 549–558. [https://doi.org/10.1016/S1004-9541\(14\)60073-2](https://doi.org/10.1016/S1004-9541(14)60073-2) (2014).
- Sajadian, S. A., Ardestani, N. S. & Jouyban, A. Solubility of montelukast (as a potential treatment of COVID-19) in supercritical carbon dioxide: Experimental data and modelling. *J. Mol. Liquids* **349**, 118219. <https://doi.org/10.1016/j.molliq.2021.118219> (2022).
- Sajadian, S. A., Ardestani, N. S., Esfandiari, N., Askarizadeh, M. & Jouyban, A. Solubility of favipiravir (as an anti-COVID-19) in supercritical carbon dioxide: An experimental analysis and thermodynamic modeling. *J. Supercrit. Fluids* **183**, 105539. <https://doi.org/10.1016/j.supflu.2022.105539> (2022).
- Esfandiari, N. & Sajadian, S. A. Experimental and modeling investigation of Glibenclamide solubility in supercritical carbon dioxide. *Fluid Phase Equilib.* **556**, 113408. <https://doi.org/10.1016/j.fluid.2022.113408> (2022).
- Amani, M., Ardestani, N. S., Jouyban, A. & Sajadian, S. A. Solubility measurement of the fludrocortisone acetate in supercritical carbon dioxide: Experimental and modeling assessments. *J. Supercrit. Fluids* **190**, 105752. <https://doi.org/10.1016/j.supflu.2022.105752> (2022).
- Iwai, Y., Fukuda, T., Koga, Y. & Arai, Y. Solubilities of myristic acid, palmitic acid, and cetyl alcohol in supercritical carbon dioxide at 35 degree C. *J. Chem. Eng. Data* **36**, 430–432. <https://doi.org/10.1021/je00004a025> (1991).
- Yamini, Y., Fat'hi, M. R., Alizadeh, N. & Shamsipur, M. Solubility of dihydroxybenzene isomers in supercritical carbon dioxide. *Fluid Phase Equilib.* **152**, 299–305. [https://doi.org/10.1016/S0378-3812\(98\)00385-9](https://doi.org/10.1016/S0378-3812(98)00385-9) (1998).
- Sodeifian, G., Sajadian, S. A. & Ardestani, N. S. Determination of solubility of Aprepitant (an antiemetic drug for chemotherapy) in supercritical carbon dioxide: Empirical and thermodynamic models. *J. Supercrit. Fluids* **128**, 102–111. <https://doi.org/10.1016/j.supflu.2017.05.019> (2017).
- Jain, A., Yang, G. & Yalkowsky, S. H. Estimation of melting points of organic compounds. *Ind. Eng. Chem. Res.* **43**, 7618–7621. <https://doi.org/10.1021/ie049378m> (2004).
- Immirzi, A. & Perini, B. Prediction of density in organic crystals. *Acta Crystallogr. Sect. A: Cryst. Phys. Diffract. Theor. General Crystallogr.* **33**, 216–218. <https://doi.org/10.1107/S0567739477000448> (1977).
- Lyman, W., Reehl, W. & Rosenblatt, D. *Research and Development of Methods for Estimating Physicochemical Properties of Organic Compounds of Environmental Concern* (McGraw Hill Book Co., 1982).
- Reid, R., Prausnitz, J. M. & Poling, B. E. The properties of gases and liquids. *Chem. Eng. Ser.* **657**, 89 (1987).
- Chrastil, J. Solubility of solids and liquids in supercritical gases. *J. Phys. Chem.* **86**, 3016–3021. <https://doi.org/10.1021/j100212a041> (1982).
- Garlapati, C. & Madras, G. Solubilities of palmitic and stearic fatty acids in supercritical carbon dioxide. *J. Chem. Thermodyn.* **42**, 193–197. <https://doi.org/10.1016/j.jct.2009.08.001> (2010).
- Méndez-Santiago, J. & Teja, A. S. The solubility of solids in supercritical fluids. *Fluid Phase Equilib.* **158**, 501–510. [https://doi.org/10.1016/S0378-3812\(99\)00154-5](https://doi.org/10.1016/S0378-3812(99)00154-5) (1999).
- Bartle, K., Clifford, A., Jafar, S. & Shilstone, G. Solubilities of solids and liquids of low volatility in supercritical carbon dioxide. *J. Phys. Chem. Ref. Data* **20**, 713–756. <https://doi.org/10.1063/1.555893> (1991).

37. Kumar, S. K. & Johnston, K. P. Modelling the solubility of solids in supercritical fluids with density as the independent variable. *J. Supercrit. Fluids* **1**, 15–22. [https://doi.org/10.1016/0896-8446\(88\)90005-8](https://doi.org/10.1016/0896-8446(88)90005-8) (1988).
38. Mahesh, G. & Garlapati, C. Correlating solubilities of some parabens in supercritical carbon dioxide using Modified Wilson's model. *Austin Chem. Eng.* **10**(1), 1096 (2023).
39. Garlapati, C. & Madras, G. Solubilities of some chlorophenols in supercritical CO<sub>2</sub> in the presence and absence of cosolvents. *J. Chem. Eng. Data* **55**, 273–277. <https://doi.org/10.1021/jc900328c> (2010).
40. Sridar, R., Bhowal, A. & Garlapati, C. A new model for the solubility of dye compounds in supercritical carbon dioxide. *Thermochim. Acta* **561**, 91–97. <https://doi.org/10.1016/j.tca.2013.03.029> (2013).
41. Ch, R. & Madras, G. An association model for the solubilities of pharmaceuticals in supercritical carbon dioxide. *Thermochim. Acta* **507**, 99–105. <https://doi.org/10.1016/j.tca.2010.05.006> (2010).
42. Reddy, S. N. & Madras, G. An association and Wilson activity coefficient model for solubilities of aromatic solid pollutants in supercritical carbon dioxide. *Thermochim. acta* **541**, 49–56. <https://doi.org/10.1016/j.tca.2012.04.025> (2012).
43. Anita, N. & Garlapati, C. A statistical analysis of solubility models employed in supercritical carbon dioxide. *AIP Conf. Proc.* **2446**, 180003. <https://doi.org/10.1063/5.0108200> (2022).
44. Zhong, M., Han, B., Ke, J., Yan, H. & Peng, D.-Y. A model for correlating the solubility of solids in supercritical CO<sub>2</sub>. *Fluid Phase Equilib.* **146**, 93–102. [https://doi.org/10.1016/S0378-3812\(98\)00207-6](https://doi.org/10.1016/S0378-3812(98)00207-6) (1998).
45. Lemert, R. M. & Johnston, K. P. Chemical complexing agents for enhanced solubilities in supercritical fluid carbon dioxide. *Ind. Eng. Chem. Res.* **30**, 1222–1231. <https://doi.org/10.1021/ie00054a024> (1991).

## Acknowledgements

Authors would like to thank the generous support provided by the research laboratory of Dr. Sajadian. Prof. G. C thank Prof. G. Madras for his inspiration and guidance.

## Author contributions

N.A., S.S., N.E. and A.R. are responsible for solubility data generation and compound selection and literature review and G.C. is responsible for modeling software. All authors reviewed the manuscript.

## Competing interests

The authors declare no competing interests.

## Additional information

**Correspondence** and requests for materials should be addressed to S.A.S. or C.G.

**Reprints and permissions information** is available at [www.nature.com/reprints](http://www.nature.com/reprints).

**Publisher's note** Springer Nature remains neutral with regard to jurisdictional claims in published maps and institutional affiliations.



**Open Access** This article is licensed under a Creative Commons Attribution 4.0 International License, which permits use, sharing, adaptation, distribution and reproduction in any medium or format, as long as you give appropriate credit to the original author(s) and the source, provide a link to the Creative Commons licence, and indicate if changes were made. The images or other third party material in this article are included in the article's Creative Commons licence, unless indicated otherwise in a credit line to the material. If material is not included in the article's Creative Commons licence and your intended use is not permitted by statutory regulation or exceeds the permitted use, you will need to obtain permission directly from the copyright holder. To view a copy of this licence, visit <http://creativecommons.org/licenses/by/4.0/>.

© The Author(s) 2023